Journal of Materials Chemistry A

COMMUNICATION

View Article Online
View Journal | View Issue

Cite this: J. Mater. Chem. A, 2018, 6, 823

Received 20th November 2017
Accepted 7th December 2017

DOI: 10.1039/c7ta10222d

rsc.li/materials-a

Radiation-induced grafting of a butyl-spacer styrenic monomer onto ETFE: the synthesis of the most alkali stable radiation-grafted anion-exchange membrane to date†

Julia Ponce-González,* Imad Ouachan, John R. Varcoe and Daniel K. Whelligan

An ETFE-(poly(ethylene-*co*-tetrafluoroethylene))-based radiation-grafted anion-exchange membrane (AEM) containing a butyl-spacer between the benzene and the methylpyrrolidinium groups (**C4-AEM**) had double the *ex situ* alkali stability at 80 °C compared to a methylene benchmark (**C1-AEM**). H_2/O_2 fuel cells containing **C4-AEM** still achieved a peak power density of >1 W cm^{-2}.

The use of aromatic polymer components in anion exchange membranes (AEMs) is widespread due to the availability of facile polymerisation and functionalisation procedures. However, the cationic head-groups that are covalently bound to benzylic positions are sensitive to substitution by hydroxide (leading to alkali unstable AEMs).[1] The major degradation products from alkali degradation of benzyltrimethylammonium cations are benzyl alcohol and trimethylamine (from direct S_N2_{Bn} mechanisms and *via* ylide formation).[2,3] A strategy to reduce degradation *via* these pathways is to introduce an aliphatic (spacer) chain between the aryl and the cationic (ion-exchanging) groups. As reviewed recently,[4] this strategy has proven successful for a wide variety of polymers containing aromatic group,[5–11] including poly(phenylene ethers), poly(phenylene) and polysulfones. In many cases, an improved ionic conductivity has also been observed on addition of spacer-groups, which was ascribed to the increased mobility of the resulting quaternary ammonium-containing side-chains.[6,12,13]

High performance AEMs containing a methylene-(C1)-group between the benzene ring and the cationic head-group have already been prepared by radiation-induced grafting of vinylbenzyl chloride (VBC) monomer onto commodity ETFE polymer films.[14] The treatment of such films in air with an e^--beam source leads to the functionalisation of the films with peroxide groups (Scheme 1).[15] Heating these radiation-activated polymer films in the presence of VBC (the grafting step) produces graft copolymers,‡ which can be subsequently functionalised with amines to yield pendant quaternary ammonium groups. These AEMs give high performances in H_2/O_2 anion-exchange membrane fuel cells (AEMFCs) but they also degrade during *ex situ* treatment in aqueous alkali solutions at >70 °C.[16–18]

We recently found that the efficiency of the grafting step could be increased by the use of water in the grating mixture.[17] However, it still remained impossible to radiation-graft linear aliphatic monomers, such as 6-chloro-1-hexene, onto ETFE, which would have eliminated the presence of base-labile benzylic groups in the resultant AEMs: radiation-grafting is a radical polymerisation process, which enables polymerisation of styrenic monomers but not linear aliphatic vinyl monomers. As a compromise solution, a styrenic monomer was selected for

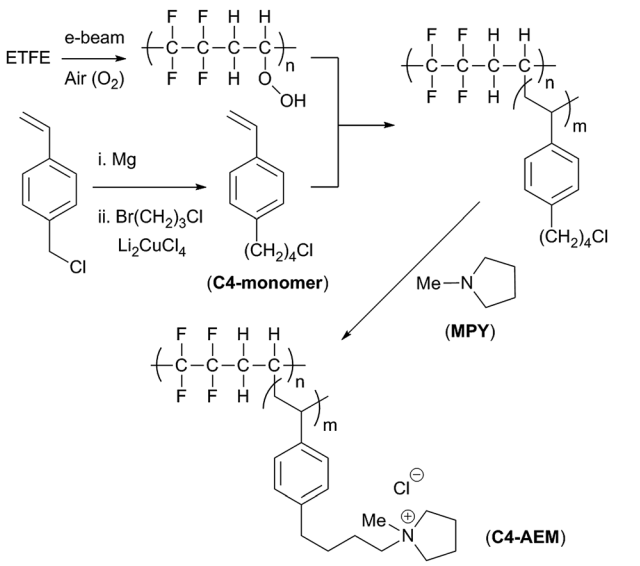

Scheme 1 An outline of the synthesis of the pyrrolidinium-grafted-ETFE-based **C4-AEM** developed in this study.‡ The **C1-AEM** benchmark contains a single $-CH_2-$ group between the benzene ring and the cationic pyrrolidinium N-atom.

Department of Chemistry, University of Surrey, Guildford GU2 7XH, UK. E-mail: jupongon@gmail.com

† Electronic supplementary information (ESI) available: Additional experimental details and data in support of the main text. See DOI: 10.1039/c7ta10222d

use that contains an alkyl-spacer-chain located between the vinylbenzene group and the cationic quaternary ammonium group: this eliminates the presence of (alkali-susceptible) benzylic quaternary ammonium groups while retaining the availability of readily-polymerizable vinylbenzene groups.

In this study, we report the synthesis of a radiation-grafted AEM containing a (C4) butyl-spacer between the aromatic and quaternary ammonium groups (**C4-AEM**), which exhibits a reduced level of alkali degradation at 80 °C. Theoretical and experimental studies on small cationic molecules have found that trimethylalkylammoniums bearing alkyl chains containing 4–6 carbon atoms in length show higher alkaline resistance than those with shorter or longer alkyl chains.[19,20] We opted for a monomer, 1-(4-chlorobutyl)-4-vinylbenzene, containing a butyl-spacer located at the *para*-aromatic position (**C4-monomer**, Scheme 1), as larger monomers (*e.g.* with a C6-spacer) risk impeded diffusion into the ETFE films in the grafting process. The bromide form of this monomer has been previously prepared by Tomoi *et al.* and converted into cross-linked quaternary ammonium anion-exchange resins.[21] The hydroxide form of these resins retained their ion exchange capacities at 100 °C more than the (C1-linked) benzyltrimethylammonium analogues. Despite the presence of C–H bonds at the β-positions to the quaternary ammonium groups, these resins did not undergo high levels of the anticipated degradation *via* Hoffman elimination.

Tomoi *et al.*'s monomer synthesis involved Cu-mediated cross-coupling of vinylbenzylmagnesium chloride with 1,3-dibromopropane.[21] We applied the same method using 1-bromo-3-chloropropane to give 4-(1′-chlorobutyl)styrene in 58% yield after distillation (details in the ESI†). A divinyl by-product (Fig. S1 in the ESI†), resulting from homocoupling of the vinylbenzylmagnesium chloride, was also present in 23% molar ratio in the crude reaction mixture: this could be reduced to 2% on distillation (calculated from the ^{1}H NMR spectra, Fig. S2 in the ESI†). This by-product can act as a crosslinker during the grafting step. Finally, 50 ppm of 4-*tert*-butylcatechol (radical polymerisation inhibitor) was added to the monomer (+2% crosslinker) mixture before use in the grafting step: this matched the inhibitor concentration in the commercially available VBC monomer (supplied as a mixture of *para*- and *meta*-isomers) used to produce the **C1-AEM** benchmark.

The grafting conditions employed were comparable to those described previously[17] but with the additional use of an ultrasound bath during the grafting step. Nasef *et al.* recently reported that the yield and kinetics of radiation-grafting could be enhanced by the use of sonication and that this additionally reduces the formation of undesired homopolymer by-products.[22] With our synthetic protocol, a comparison between ultrasound-aided and ultrasound-free radiation-grafting of VBC indicated that the use of ultrasound did not improve grafting yield but did allow a reduction in grafting time (6 h with sonication *vs.* 16 h without) with the elimination of poly(VBC) homopolymer formation (previously observed as a white solid on the walls of the grafting vessel). The **C4-monomer** also underwent ultrasound-assisted radiation-grafting but resulted in lower grafting yields compared to the VBC, due to its higher molecular weight. Non-ultrasound grafting of **C4-monomer** was even less successful and led to high levels of undesired homopolymer (confirmed by Raman spectroscopy, see Fig. S3 in the ESI†).

The optimum conditions for grafting **C4-monomer** onto ETFE films (yielding **ETFE-polyC4**) involved immersion of pre-irradiated ETFE (40 kGy in air) in N_2-purged monomer–water mixtures containing the wetting agent 1-octyl-2-pyrrolidone (1% vol) and heating for 6 h at 70 °C with sonication (35 kHz, 225 W). To account for the 28% higher molecular weight of **C4-monomer**, it was used at a concentration of 5% vol, while 4% vol VBC was used to synthesise the **ETFE-polyVBC** membrane that was then aminated to form the **C1-AEM** benchmark (all other grafting conditions were identical). Grafting was confirmed using Raman spectroscopy where significant differences were observed between the two monomers (Fig. 1). The benzylic CH_2Cl deformation (1270 cm^{-1}) was not visible in the spectrum of **ETFE-polyC4**. The bands characteristic of *meta*-disubstituted benzene rings (1000 cm^{-1} and 700 cm^{-1}) were also absent,[16,23] since the **C4-monomer** was synthesised from a *para*-disubstituted-only starting material. Homogeneous grafting, throughout the core of both pre-aminated membranes, was confirmed by cross-sectional Raman maps of the ratio between the areas of the 1615 cm^{-1}/830 cm^{-1} bands, since these represent the aromatic ring/ETFE components, respectively (see Fig. S4 in the ESI†).[16,24]

For the amination of **ETFE-polyVBC** and **ETFE-polyC4**, to form **C1-AEM** and **C4-AEM** respectively, we selected *N*-methylpyrrolidine (MPY): this yields AEM cationic head-groups with superior alkaline stabilities and enhanced fuel cell performances compared to the traditional use of trimethylamine (TMA).[16] We suspect that the reason behind the enhanced *ex situ* stability of MPY membranes is related to their higher λ_{water} (average number of H_2O molecules per anion), being around 1.5 times those of TMA-based AEMs.[18] As recently published, the number of water molecules solvating the OH^- anions has a substantial effect on AEM chemical stability.[25,26] Furthermore, attempts to aminate **ETFE-polyC4** at room temperature with TMA proved unsuccessful due to the higher activation energies required for S_N2 reactions on non-benzylic primary alkyl chlorides (the high volatility of aqueous TMA solutions impedes the

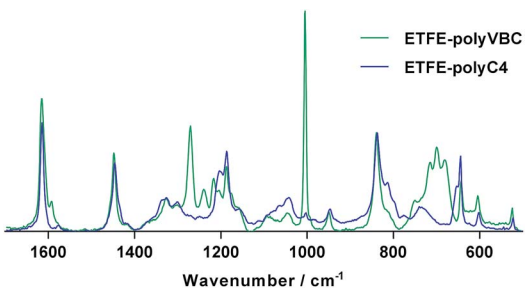

Fig. 1 Raman spectra of the pre-aminated radiation-grafted ETFE-films synthesised using the C4-monomer and commercially available VBC (*meta*- and *para*-isomer mixture). All spectra have been normalized to the 830 cm^{-1} band (related to the ETFE backbone) to aid visual comparison. Laser $\lambda = 532$ nm.

use of elevated temperatures on safety grounds). A prior optimisation study for the MPY amination of **ETFE-polyVBC** intermediates concluded that using 15% vol MPY in water for 6 hours at 60 °C was the mildest and cheapest effective option (details in the ESI†). However, this did not translate to **ETFE-polyC4** (containing lower reactivity, non-benzyl head-groups): 70 °C and 24 h were required with the use of aqueous MPY (15% vol).

C4-AEM had 20% lower ion-exchange capacity (IEC) than the **C1-AEM** benchmark due to its lower Degree of Grafting (DoG) (Table 1). However, the Water Uptakes (WU) and λ_{water} values were similar for both AEMs. Likewise, no major differences in the swelling degrees and the mechanical properties were seen between the two AEMs (Tables 1, S2, Fig. S6 and S7 in the ESI†). The Cl^- conductivity of **C4-AEM** was lower than that of **C1-AEM** (Table 1 and Fig. S5 in the ESI†) but, as expected for AEMs containing similar pyrrolidinium chemistries and λ_{water} values, the IEC-normalised conductivities[27] were similar (Fig. 2).

The H_2/O_2 AEMFC performances at 60 °C of membrane electrode assemblies (MEA) comprising both AEMs were evaluated using gas diffusion electrodes (GDEs) that contained 20% wt ETFE-benzyltrimethylammonium-based anion-exchange ionomer powder[28] and 80% wt electrocatalysts: the Pt/C cathodes and PtRu/C anodes (all 0.40 ± 0.01 mg_{Pt} cm^{-2}) were prepared as previously reported (details in the ESI†).[18] The low current performances of both AEMs were identical, confirming similar electrocatalytic activities (Fig. 3). However, the performance curves deviate at higher currents, where internal ohmic resistances and mass transport losses control performances. **C1-AEM** achieved a peak power density of 1.22 W cm^{-2}, whereas **C4-AEM** obtained 1.02 W cm^{-2} (under identical test conditions): this 17% lower power density is still good considering **C4-AEM** was 26% lower in conductivity at 60 °C than **C1-AEM**. The peak power increased to 1.12 W cm^{-2} at 70 °C with **C4-AEM** but no further improvement was observed when raising the temperature to 80 °C (Fig. S8 in the ESI†).

The *ex situ* chemical stabilities were tested by ageing individual samples of each AEM in aqueous KOH (1 mol dm^{-3}) at

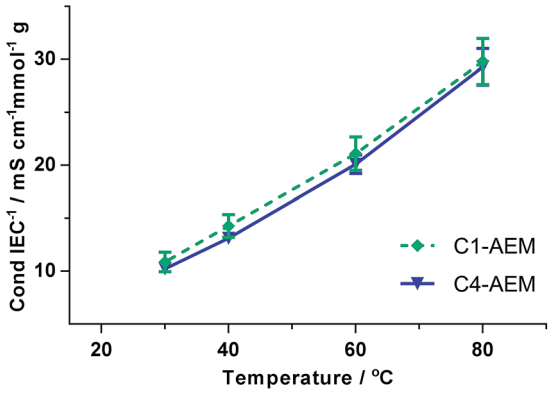

Fig. 2 IEC-normalised Cl^--anion conductivities (4-probe, in-plane, measured in water). Errors bars are from repeat measurement on $n = 3$ samples of each AEM.

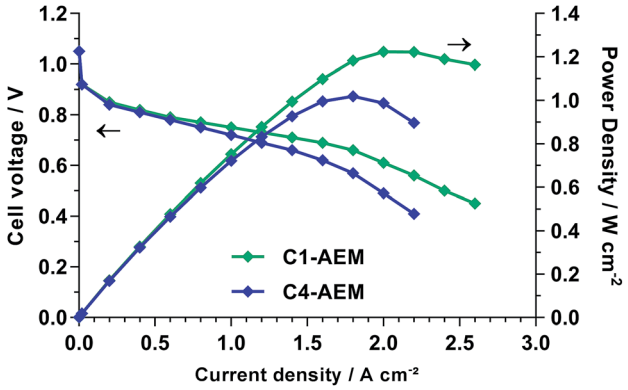

Fig. 3 H_2/O_2 fuel cell performances at 60 °C with PtRu/C anodes and Pt/C cathodes (all 0.4 mg_{Pt} cm^{-2}). The unpressurised gases were supplied at 1 SLPM and 68% RH.

Table 1 Key properties of both radiation-grafted AEMs studied (errors are from repeat measurement on $n = 3$ or 4 samples of each AEM: n indicated in brackets)

	C1-AEM	C4-AEM
DoG (%)	75	66
IEC/mmol g^{-1}	1.92 ± 0.05(4)	1.508 ± 0.005(4)
WU (%)	95 ± 12(4)	85 ± 8(4)
λ_{water} [a]	28 ± 3(4)	31 ± 3(4)
SD_{xy} (%)[b]	51 ± 5(3)	52 ± 1(3)
SD_z (%)[c]	65 ± 6(3)	59 ± 8(3)
σ_{Cl} (60 °C)/mS cm^{-1}[d]	41 ± 3(3)	30.4 ± 1.3(3)

[a] Average number of H_2O molecules per Cl^- anion calculated as: λ_{water} = WU (%)/(100 × 18.02 × IEC), where IEC is in mol g^{-1}. [b] Swelling degree in the x–y (in-plane) direction. [c] Swelling degree in the z (through-plane, thickness) direction. [d] The Cl^- anion conductivities at 60 °C of the fully hydrated AEMs (4-probe, in-plane measurements with the RG-AEM submerged in water).

80 °C for 28 d. Post-aged samples were converted back into the Cl^--form and the IECs were re-measured (Table 2). The loss of IEC with **C4-AEM** was half that of the **C1-AEM** benchmark. For more insights into the degradation mechanisms, CHN + Cl elemental analyses were also performed (Fig. 4). The % Cl loss correlates with the % IEC loss as all degradation mechanisms lead to loss of Cl^- anions. However, the differences between the % Cl and % N losses indicate multiple degradation mechanisms are operating (discussed previously:[16] see Fig. S9 in the ESI†).

Around a third of the degradation of **C1-AEM** involves loss of the N atoms due to OH^- derived displacement of complete MPY head-groups (S_N2_{Bn}). Degradation by this pathway is essentially eliminated with **C4-AEM**, as the partial negative charges on the α-C atom (attached to the quaternary ammonium N) are not stabilized by resonance with a phenyl ring (confirms the stabilising effect of the spacer-group).[4] For **C4-AEM**, degradation *via* Hoffman elimination at the spacer-chain is also possible, which would lead to loss of N content: however, the near zero % N loss indicates that this, along with nucleophilic loss of MPY, does not occur to a significant extent (in accordance with Tomoi *et al.*).[21] Adding a spacer-chain appears to have "switched

Table 2 The IEC values of AEM samples ($n = 4$) recorded before and after *ex situ* alkali ageing in aqueous KOH (1 mol dm^{-3}) at 80 °C for 28 d

	C1-AEM	C4-AEM
IEC pre-aged AEM/mmol g^{-1}	1.88 ± 0.03	1.44 ± 0.04
IEC post-aged AEM/mmol g^{-1}	1.38 ± 0.01	1.25 ± 0.02
IEC loss (%)	27 ± 2	13 ± 3

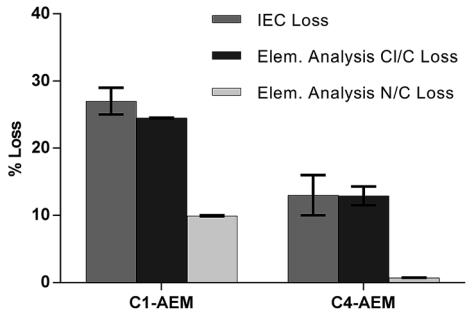

Fig. 4 % loss of IEC and % losses of Cl/C and N/C molar ratios, the latter extracted from elemental analyses, of the AEM samples before and after *ex situ* alkali treatment in aqueous KOH (1 M) at 80 °C for 28 days.

off" the degradation mechanisms involving loss of N atoms (see the degradation mechanisms in Fig. S9 in the ESI†). Nevertheless, 13% degradation still occurs with **C4-AEM**, which is predominantly due to loss of positive charges (loss of Cl^- anions) but with retention of N atoms on the polymer grafts. This can proceed *via* nucleophilic substitution on the *N*-methyl group (S_N2_{NMe}) or ring-opening of the 5-membered heterocyclic ring.[29] A previous study of ETFE-based VBC-grafted AEMs, with different head-groups,[16] observed 12–14% degradation that did not involve loss of N content (approximately constant for TMA-, MPY- and *N*-methylpiperidinium-based head-groups). To obtain further confirmation of the degradation mechanisms, solid-state ^{13}C and ^{14}N NMR spectra were recorded on the pre- and post-alkali-aged samples, but no discernible changes were observed on ageing (see Fig. S10 and S11 in the ESI†).

Conclusions and future research directions

The introduction of a (C4) butyl-spacer between the quaternary ammonium and the benzene rings of a ETFE-based radiation-grafted anion-exchange membrane (AEM) led to a significant enhancement in *ex situ* alkali stability (compared to the non-spacer methylene-(C1)-linked benchmark). A more realistic evaluation of chemical stability would involve alkali treatment of AEM samples at low relative humidity since, as recently reported, dehydration of the cathode during fuel cell operation accelerates degradation of the polymer electrolytes.[25,26,30] These experiments will be considered for future, more extensive studies on these AEMs. The additional use of ultrasound during the grafting step was essential for successful synthesis of the new **C4-AEM**. A lower degree of grafting (*cf.* the C1-benchmark) led to a decrease in conductivity and fuel cell performance (peak power densities still exceeded 1 W cm^{-2}). Next steps involve increasing the ion-exchange capacity (degree of grafting) of the C4-spacer AEMs and development of a C4-type radiation-grafted anion-exchange ionomer powder to enable *in situ* fuel cell durability studies with spacer-only anion-exchange polymer electrolytes in the membrane electrode assemblies (the lack of spacer-type ionomer powders currently precludes *in situ* durability studies as the current non-spacer ionomer powder degrades faster).

Data access

All raw data is freely available on request: access details can be found at DOI: 10.15126/surreydata.00845195.

Conflicts of interest

There are no conflicts of interest to declare.

Acknowledgements

The research was funded by EPSRC grant EP/M005933/1. Imad thanks the University of Surrey for providing funds for his undergraduate final year project.

Notes and references

‡ It is not currently known whether an oxygen atom (C–O–C ether group) links the ETFE backbone and the pendent grafted polymer chains or if the link is a C–C bond.[15]

1 S. A. Nuñez, C. Capparelli and M. A. Hickner, *Chem. Mater.*, 2016, **28**, 2589.
2 A. D. Mohanty and C. Bae, *J. Mater. Chem. A*, 2014, **2**, 17314.
3 M. R. Sturgeon, C. S. Macomber, C. Engtrakul, H. Long and B. S. Pivovar, *J. Electrochem. Soc.*, 2015, **162**, F366.
4 P. Jannasch and E. A. Weiber, *Macromol. Chem. Phys.*, 2016, **217**, 1108.
5 H.-S. Dang and P. Jannasch, *Macromolecules*, 2015, **48**, 5742.
6 Z. Yang, J. Zhou, S. Wang, J. Hou, L. Wu and T. Xu, *J. Mater. Chem. A*, 2015, **3**, 15015.
7 L. Zhu, J. Pan, Y. Wang, J. Han, L. Zhuang and M. a. Hickner, *Macromolecules*, 2016, **49**, 815.
8 M. R. Hibbs, *J. Polym. Sci., Part B: Polym. Phys.*, 2013, **51**, 1736.
9 J. Han, Q. Liu, X. Li, J. Pan, L. Wei, Y. Wu, H. Peng, Y. Wang, G. Li, C. Chen, L. Xiao, J. Lu and L. Zhuang, *ACS Appl. Mater. Interfaces*, 2015, **7**, 2809.
10 W. H. Lee, Y. S. Kim and C. Bae, *ACS Macro Lett.*, 2015, **4**, 814.
11 C. Xiao Lin, X. Qin Wang, E. Ning Hu, Q. Yang, Q. Gen Zhang, A. Mei Zhu and Q. Lin Liu, *J. Membr. Sci.*, 2017, **541**, 358.
12 H.-S. Dang, E. A. Weiber and P. Jannasch, *J. Mater. Chem. A*, 2015, **3**, 5280.

13 C. X. Lin, X. L. Huang, D. Guo, Q. G. Zhang, A. M. Zhu, M. L. Ye and Q. L. Liu, *J. Mater. Chem. A*, 2016, **4**, 13938.
14 J. R. Varcoe, R. C. T. Slade, E. Lam How Yee, S. D. Poynton, D. J. Driscoll and D. C. Apperley, *Chem. Mater.*, 2007, **19**, 2686.
15 L. Gubler, *Adv. Energy Mater.*, 2014, **4**, 1300827.
16 J. Ponce-Gonzalez, D. K. Whelligan, L. Wang, R. Soualhi, Y. Wang, Y. Peng, H. Peng, D. C. Apperley, H. N. Sarode, T. P. Pandey, A. G. Divekar, S. Seifert, A. Herring, L. Zhuang and J. R. Varcoe, *Energy Environ. Sci.*, 2016, **9**, 3724.
17 L. Wang, E. Magliocca, E. L. Cunningham, W. E. Mustain, S. D. Poynton, R. Escudero-Cid, M. M. Nasef, J. Ponce-González, R. Bance-Souahli, R. C. T. Slade, D. K. Whelligan and J. R. Varcoe, *Green Chem.*, 2017, **19**, 831.
18 L. Wang, J. J. Brink, Y. Liu, A. M. Herring, J. Ponce-González, D. K. Whelligan and J. R. Varcoe, *Energy Environ. Sci.*, 2017, **10**, 2154.
19 H. Long and B. S. Pivovar, *J. Phys. Chem. C*, 2012, **116**, 9419.
20 M. G. Marino and K. D. Kreuer, *ChemSusChem*, 2015, **8**, 513.
21 M. Tomoi, K. Yamaguchi, R. Ando, Y. Kantake, Y. Aosaki and H. Kubota, *J. Appl. Polym. Sci.*, 1997, **64**, 1161.
22 M. M. Nasef, P. Sithambaranathan, A. Ahmad and E. Abouzari-lotf, *Radiat. Phys. Chem.*, 2017, **134**, 56.
23 P. Larkin, *Infrared and Raman Spectroscopy; Principles and Spectral Interpretation*, Elsevier Science, 2011.
24 W. H. Lee, C. Crean, J. R. Varcoe and R. Bance-Soualhi, *RSC Adv.*, 2017, **7**, 47726.
25 D. R. Dekel, M. Amar, S. Willdorf, M. Kosa, S. Dhara and C. E. Diesendruck, *Chem. Mater.*, 2017, **29**, 4425.
26 D. R. Dekel, S. Willdorf, U. Ash, M. Amar, S. Pusara, S. Dhara, S. Srebnik and C. E. Diesendruck, *J. Power Sources*, 2017, **375**, 351.
27 S. Gu, R. Cai and Y. Yan, *Chem. Commun.*, 2011, **47**, 2856.
28 S. D. Poynton, R. C. T. Slade, T. J. Omasta, W. E. Mustain, R. Escudero-Cid, P. Ocón and J. R. Varcoe, *J. Mater. Chem. A*, 2014, **2**, 5124.
29 X. Dong, D. Lv, J. Zheng, B. Xue, W. Bi, S. Li and S. Zhang, *J. Membr. Sci.*, 2017, **535**, 301.
30 K. D. Kreuer and P. Jannasch, *J. Power Sources*, 2017, **375**, 361.